Spatial Fourier-decomposition optical fluorescence tomography-theoretical investigation

Cheng Liu (刘 诚)[1,2,3], Dug Young Kim[2], and Jianqiang Zhu (朱健强)[3]

[1]*Physics Department of Xuzhou Normal University, Xuzhou 221009*

[2]*Gwangju Institute of Science and Technology, Gwangju, South Korea*

[3]*Shanghai Institute of Optics and Fine Mechanics, Chinese Academy of Sciences, Shanghai 201800*

Received July 15, 2008

A new three-dimensional (3D) optical fluorescent tomographic imaging scheme is proposed with structured illumination and spatial Fourier-domain decomposition methods for the first time. In this spatial Fourier-decomposition optical fluorescence tomography (SF-OFT), the intensity of focused excitation light from an objective lens is modulated to be a cosine function along the optical axis of the system. For a given position in a two-dimensional (2D) raster scanning process, the spatial frequency of the cosine function along the optical axis sweeps in a proper range while a series of fluorescence intensity are detected accordingly. By making an inverse discrete cosine transformation of these recorded intensity profiles, the distribution of fluorescent markers along the optical axis of a focused laser beam is obtained. A 3D optical fluorescent tomography can be achieved with this proposed SF-OFT technique with a simple 2D raster scanning process.

OCIS codes: 110,0110, 070.0070.

doi: 10.3788/COL20080609.0665.

Despite its limitation in spatial resolution, light microscopy is one of the most powerful tools used in bioscience especially for studying the structure and the function of a live cell. Lately, various laser-based optical microscopic imaging techniques have been developed and used widely in many applications. Among them, optical fluorescence-based functional microscopy such as fluorescence lifetime imaging microscopy (FLIM) or fluorescent resonant energy transfer (FRET) microscopy has attracted much attention due to its capability for monitoring individual molecules, observing protein-protein interactions, and imaging ion concentration or pH value in a live cell[1]. In most optical microscope systems, three-dimensional (3D) sectioning and display is one of the most difficult and time-consuming obstacle to be overcome for real-time observation of molecular interactions in a live cell, drug delivery procedure in pharmaceutical research, and many other biomedical applications. Optical coherence tomography (OCT) has shown great achievement in 3D optical imaging.

Great achievement has been made lately in 3D biomedical imaging by OCT, which uses a coherence gating scheme to identity the axial position of a light scattering object along the propagation direction of a focused laser light[2,3]. Since the lens of high numerical aperture is not needed for coherence gating, OCT can see much deeper into the sample than 3D confocal microscopy, and it has been widely employed in dermatology and ophthalmic examination. Since standard OCT can only retrieve the physical structure of a specimen (for example, index or layer distribution) and is lack of identifying specific chemicals, proteins, or lipids, there are great needs and efforts for the development of 3D fluorescence microscopy. Even though the fluorescence microscopy is a well developed and widely used optical method in biology with the help of fluorescent labeling technology, a practical real-time fluorescence tomography is not available yet, and lots of approaches with various new ideas have been suggested for this purpose. Fluorescence diffuse optical tomography (FDOT) and fluoresce coherence tomography (FCT) are two major techniques of this kind[4−7]. FDOT reconstructs the structure of a specimen from the diffused fluorescence based on an optimization strategy[4−6]. In FCT, the depth information of a sample is retrieved by detecting the self-interference of fluorescence light from a fluorescence maker with an imaging spectrometer composed of two opposing low-NA objective lenses[7,8].

However, due to high incoherency, low intensity of the emitted fluorescent light, and diffusion, the performance of these two techniques are still not very satisfying in terms of resolution and signal-to-noise ratio compared with standard OCT or conventional fluorescence microscopy. When compared with excitation light, emitted fluorescence is normally much weaker in FCT. And due to the high incoherency of emitted light, it is difficult to be collimated or coupled into a fiber for detection. These are major difficulties to use the coherence gate technique for fluorescent light. To circumvent these problems, we propose spatial Fourier-decomposition optical fluorescence tomography (SF-OFT) based on structured illumination and spatial Fourier decomposition method, which can make real-time fluorescence tomographic imaging possible. Instead of using interference between reference and reflected lights for obtaining the depth information of a fluorescence maker, the spatial distribution of fluorescent markers along the axial direction of a focused laser beam is obtained by using spatial Fourier decomposition method. As no interference signal is used, the SF-OFT system is very simple and suitable for practical application.

The principle of SF-OFT is schematically shown in

 © 2008 Chinese Optics Letters

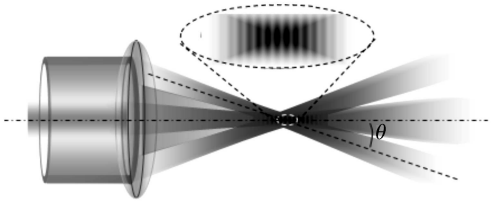

Fig. 1. Formation of the structured focus.

Fig. 1, where light incidents into an objective lens composed of two parts. One is a circular laser beam whose diameter is much smaller than that of the objective lens coming into the center of the objective lens, and the other is a donut shape annular laser beam. Both of them are polarized in the same direction (x-direction in this example). When the diameter of the circular beam is small enough compared with that of an objective lens, it can be regarded as a plan wave near the geometrical focal point of the lens with a wave number of $k_z = k_0 = \frac{2\pi}{\lambda}$, and the electric field distribution along the optical axis z can be approximated as

$$E_{x1} = E_1 \cos(wt + k_0 z). \quad (1)$$

The annular incident beam will be focused into a shape of empty cone with a cone-angle of $\theta = \tan^{-1}(0.5D/f)$, where D is the central diameter of the annular incident beam, f is the focal length of the objective lens. Due to the symmetry of the incident beam, the field distribution of the focused annular beam around the geometrical focal point can be approximately written in the following form along the optical axis:

$$E_{x2} = E_2 \cos(wt + k_0 \cos\theta z). \quad (2)$$

The overall electric field of the two incident beams along the optical axis near the geometrical focal point of the lens can be written as

$$E_x = E_1 \cos(wt + k_0 z) + E_2 \cos(wt + k_0 \cos\theta z). \quad (3)$$

By adjusting the diameter of the central circular beam, we can have $E_2 = E_1 = E_0$, then we have

$$E_x = E_0[\cos(wt + k_0 z) + \cos(wt + k_0 \cos\theta z)]$$

$$= 2E_0 \cos[wt + k_0 z(1 + \cos\theta)] \cos[k_0 z(1 - \cos\theta)]. \quad (4)$$

From this, the intensity of light along the optical axis near the focal point can be obtained as

$$I_x = |E_x|^2 = 4E_0^2 \cos^2[k_0 z(1 - \cos\theta)]. \quad (5)$$

As illustrated in Fig. 1, the structure of light intensity around the geometric focal point along the optical-axis becomes sinusoidal whose period is determined by the conic angle θ of the focused conical beam. In SF-OFM, this periodic structured laser beam is used for exciting fluorescence markers near the focal point of an objective lens in a sample, and the fluorescent light emitted by these markers is collected by another lens. We can control the period or the spatial frequency of the sinusoidal excitation laser beam intensity near the focal point by changing the diameter D of the incident annular beam. A series of emitted fluorescence lights are collected for many excitation laser beams with different spatial frequencies. The structure of spatial distribution of fluorescence markers in a sample along the optical axis can be obtained, that is, by using a Fourier decomposition method by using fluorescent light intensities collected for a series of different spatial frequencies.

In the above discussions, only rough analysis is used to explain the main principle of SF-OFM. For the precise analysis of the intensity distribution of the excitation laser beam near the focal point of an objective lens, we have adapted accurate vector formula shown in Ref. [9]. Intensity distributions near the focal point of the objective lens are calculated with the vector diffraction formula as shown in Figs. 2(a)—(d) for four different conic angles of $\theta = 7°$, $11°$, $15°$, and $20°$ respectively. In these calculations, the numerical aperture of the central circular incident beam is assumed to be 0.15. For each conic angle θ, the width (the difference between inner and the outer diameter of the annular beam) of the annular beam decreases by $1/\sin(2\theta)$ to keep the energy of the two different beams to be equal. It should be noted that the complex intensity distribution of incident light in front of the objective lens shown in Fig. 1 could be easily realized by using a programmable spatial light modulator placed just before the objective lens[10]. Figure 2 clearly shows that light intensity near the focal point is periodic along the optical axis and its spatial frequency increases with θ. On the other hand, the width of the central lobe decreases with θ.

In fluorescence microscopy, the emitted fluorescence light from a fluorophore at a given spatial position z is considered to be proportional to the intensity of exciting field $|E_x|^2$ and the density of fluorophore $\alpha(z)$[11]. Then, the overall power of generated fluorescence light along the optical axis can be written as

$$I_{\rm det} = \int \alpha(z) |E_x|^2 {\rm d}z$$

$$= 4E_0^2 \int \alpha(z) \cos^2[k_0 z(1 - \cos\theta)] {\rm d}z$$

$$= 2E_0^2 \int \alpha(z) {\rm d}z + 2E_0^2 \int \alpha(z) \cos[k_0 z(1 - \cos\theta)] {\rm d}z. \quad (6)$$

Let $k_0(1 - \cos\theta) = k_\theta$, Eq. (6) can be written as

$$I_{\rm det}(k_\theta) = 2E_0^2 \int \alpha(z) {\rm d}z + 2E_0^2 \int \alpha(z) \cos[k_\theta z] {\rm d}z. \quad (7)$$

The second term in Eq. (7) is essentially the cosine

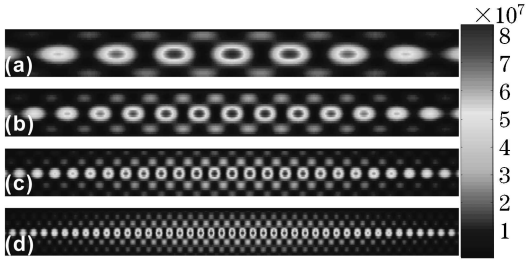

Fig. 2. Structured focus with different modulation frequencies. (a) $\theta = 7°$; (b) $\theta = 11°$; (c) $\theta = 15°$; (d) $\theta = 20°$.

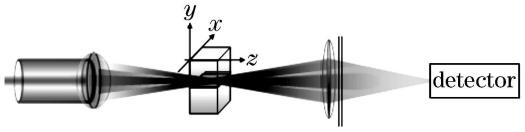

Fig. 3. Simulated setup.

transform of spatial fluorophore density function $\alpha(z)$. In experiment, the overall power of generated fluorescence light along the optical axis $I_{\rm det}(k_\theta)$ can be collected by using a second objective lens shown in Fig. 3. A series of $I_{\rm det}$ can be collected by changing θ in Fig. 1 and by making a discrete inverse cosine transform we can obtain the spatial distribution of the fluorophore $\alpha(z)$. Note that the first term in Eq. (7) is just a constant offset and does not change with θ. Since its cosine transform contributes only at the origin, the contribution by this term can be numerically subtracted without making no influence on the reconstruction of spatial fluorophore density function $\alpha(z)$. Furthermore, the value of this term is two times of the fluorescence power generated by the central beam alone, therefore it can be directly measured and subtracted in practical experiments.

In order to verify the feasibility of our suggested SF-OFM, a numerical simulation is done for a possible setup shown in Fig. 3. Periodically structured light illumination near the focal point of a lens has been used to excite fluorescence markers in a sample. Raster scanning is assumed to be realized by moving a sample stage in the x-y plane. Another objective lens is supposed to collect fluorescence light from the sample in the forward direction, forming a confocal system with the illumination objective lens. In the simulation, the numerical aperture of the illumination objective lens is assumed to be 0.6 and the effective numerical aperture of the central thin incident beam is 0.15. The numerical aperture of the collecting objective lens is assumed to be 0.2. Note that the numerical aperture of the collecting objective lens is chosen to be much smaller than that of the illuminating objective lens to suppress unwanted fluorescence lights from off-axis positions. To have a series of k_θ increasing with a constant interval, θ in Fig. 1 is varied with $\theta_n = a\cos(0.0033n)$, where $n = 211, 212, \cdots, 300$. In other words, k_θ is varied for 90 different k_θ values with a constant interval $\Delta k_\theta = 0.0033k_0$. At each position during the raster scanning of the sample, an sample is exposed with these 90 different periodic structured excitation lights successively and the powers of emitted fluorescence lights for each excitation light are collected by the collecting objective lens. According to Eq. (7), the spatial distribution function of the fluorophore $\alpha(z)$ can be obtained by making a discrete cosine transform. Two-dimensional (2D) image in the x-z coordinate space can be obtained with our proposed SF-OFM scheme by doing a single transverse scan along the x-axis as shown in Fig. 3. Figure 4(a) shows the distribution of fluorophores in a sample to be imaged by SF-OFM in the x-z plane: $\alpha(x, z)$. When this is illuminated with a periodically structured excitation laser beam with a given value of k_θ, we have one measured value of fluorescence power denoted as $I_{\rm det}(x, k_\theta)$. Figure 4(b) displays simulated data of detectable intensity $I_{\rm det}(x, k_\theta)$. By making a one-

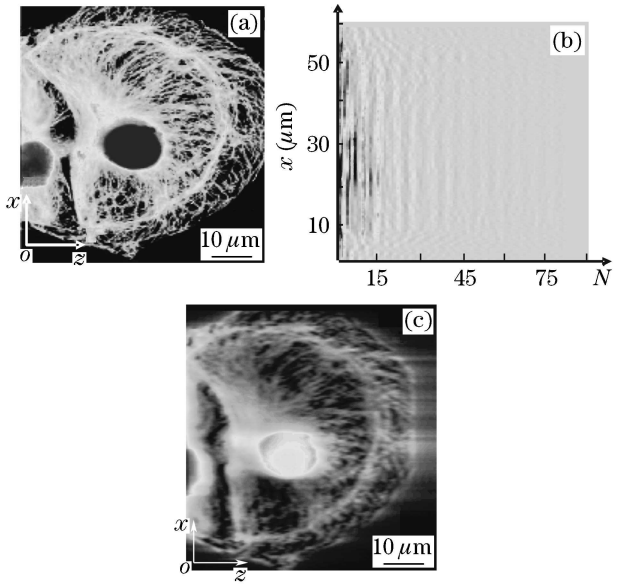

Fig. 4. (a) Original density distribution of the fluophor; (b) matrix of the detected fluorescence energy; (c) reconstructed fluophor density distribution.

dimensional cosine discrete transform for the fluorescence matrix of $I_{\rm det}(x, k_\theta)$ shown in Fig. 4(b), 2D function of fluorophore $\alpha'(x, z)$ is reconstructed and is shown in Fig. 4(c). Here, the zero-order continuous-wave (CW) component related to the first term in Eq. (7) has been filtered out for better image quality and contrast. Compared with the original distribution of $\alpha(x, z)$ shown in Fig. 4(a), the calculated fluorophore distribution function of $\alpha'(x, z)$ displayed in Fig. 4(c) is satisfying. Although there is some degradation in the spatial resolution in some degree, most of the details of the original fluorophore distribution are clearly reconstructed.

In conclusion, we have proposed and numerically demonstrated the principle of SF-OFT. The intensity of excitation light near the focal point of an objective lens can be modulated into a grating-like structure along the optical-axis by using a small circular beam at the center of an objective lens combined with a concentric annular beam in front of the objective lens. When this kind of structured beam is used for exciting fluorophores distributed with a function of $\alpha(z)$ in a sample, we can measure fluorescence power $I_{\rm det}(k_\theta)$ collected by another objective lens with a low numerical aperture in confocal geometry with respect to the illumination objective lens. This measured fluorescence power varies with the spatial frequency of the structured excitation beam k_θ. By sweeping the spatial frequency at each transverse position of the sample, the distribution of fluorophores density $\alpha'(z)$ can be reconstructed by making a inverse discrete cosine transform. By numerical simulation, we have demonstrated that the quality of the reconstructed image by our proposed SF-OFT is very satisfying. Since there is no interference used in this method and only the fluorescence power is detected, the system based on this method should be very simple and stable making this SF-OFT more suitable for practical applications. In this letter, the scanning of the spatial frequency of grating-like excitation laser beam is realized by changing the diameter of the annular beam. However, the spatial frequency

can be scanned very fast by using a swept laser source for the exciting beam, the spatial frequency can be realized by changing k_0 in Eq. (5). Furthermore, though the main content of this letter is focused on the application of the optical fluorescence tomography, we believe that our structured excitation scheme combined with Fourier decomposition method can be used for many other tomographic measurement applications.

This work was supported by Creative Research Initiatives (3D Nano Optical Imaging System Research Group) of MOST/KOSEF. C. Liu's e-mail address is liucheng96@hotmail.com.

References

1. D. J. Stephens and V. J. Allan, Science **300,** 82 (2003).
2. D. Huang, E. A. Swanson, C. P. Lin, J. S. Schuman, W. G. Stinson, W. Chang, M. R. Hee, T. Flotte, K. Gregory, C. A. Puliafito, and J. G. Fujimoto, Science **254,** 1178 (1991).
3. A. F. Fercher, W. Drexler, C. K. Hitzenberger, and T. Lasser, Rep. Prog. Phys. **66,** 239 (2003).
4. M. J. Eppstein, D. J. Hawrysz, A. Godavarty, and E. M. Sevick-Muraca, Proc. Nat. Acad. Sci. **99,** 9619 (2002).
5. R. Roy, A. B. Thompson, A. Godavarty, and E. M. Sevick-Muraca, IEEE Trans. Med. Imaging **24,** 137 (2005).
6. J. Wu, Y. Wang, L. Perleman, I. Itzkan, R. R. Desai, and M. S. Feld, Opt. Lett. **20,** 489 (1995).
7. A. Bilenca, A. Ozcan, B. Bouma, and G. Tearney, Opt. Express **14,** 7134 (2006).
8. K. E. Drabe, G. Cnossen, and D. A. Wiersma, Opt. Commun. **73,** 91 (1989).
9. S. Y. Hasegawa, N. Aoyama, A. Futamata, and T. Uchiyama, Appl. Opt. **38,** 2297 (1999).
10. L. Liu, C. Liu, W. C. Howe, C. J. R. Sheppard, and N. Chen, Opt. Lett. **32,** 2375 (2007).
11. Mats G. L. Gustafsson, PNAS **102,** 13081 (2005).